Statistical Modeling of Interactions between Gas Molecules and Pulsed Optical Lattices

C. Ngalande*, S. Gimelshein* and M. Shneider†

*University of Southern California, Los Angeles, CA 90089
†Princeton University, Princeton, NJ 08544

Abstract. The direct simulation Monte Carlo method is used to investigate interaction of an optical lattice created by two counter-propagating laser fields with gas molecules. Trapping of molecules by an optical lattice potential in the collisional regime is shown. Energy and momentum deposition from lattice to gas is examined, and the ability of a lattice to increase gas temperature to thousands of K in a single pulse is demonstrated. The formation and evolution of an acoustic signal created by the lattice is examined.

Keywords: Surface roughness, rarefied gas flows, DSMC, mass flow measurements
PACS: 51.10.+y, 51.90.+r

INTRODUCTION

An optical lattice is created by two intersecting counter propagating laser fields, and is characterized by an interaction between polarizable particles and the field of the optical interference pattern. With increasing laser beam intensities, the optical lattice potential depth increases and at relatively low gas densities a large number of gas particles can be trapped and accelerated [1]. Such hyperthermal molecular beams are of great importance for material processing such as etching, deposition, as well as for studying the relaxation processes in gases and gas-surface interactions.

The main objective of this work is to study the interaction of a pulsed optical lattice with gas molecules in the flow regimes from free molecular to near-continuum and, in particular, examine the impact of lattice and gas properties. Two applications will be considered, energy and momentum deposition from optical lattice to molecular gases, and the propagation of an acoustic wave created by an optical lattice. The direct simulation Monte Carlo (DSMC) [2] based software system SMILE [3] was used in all computations.

THEORETICAL BACKGROUND

It has been shown [1] that the equation of motion of a particle moving in a pulsed accelerated or decelerated optical lattice is given by

$$\frac{d^2x}{dt^2} = -\frac{1}{2}[\alpha q E_1(t) E_2(t)/m]\sin(qx - \beta t^2), \tag{1}$$

where α is the molecular polarizability, q is the wave number, E_1 and E_2 are the amplitudes of the electric fields of the two laser beams, m is the particle mass, and β is the frequency chirp. In a reference frame that accelerates with the optical lattice, this equation may be conveniently re-written in non-dimensional units,

$$\frac{d^2\theta}{dT^2} = -\frac{aq}{\beta}\sin(\theta) - 2, \tag{2}$$

where $\theta = X - T^2$ is the phase of the particle with respect to the accelerated frame, and $T = \sqrt{\beta}t$ and $X = qx$ are the nondimensional temporal and spatial variables, respectively. The phase space analysis [1] shows that particles may be trapped when the requirement $\left|\frac{2\beta}{aq}\right| < 1$ is satisfied; in this case, particle velocities increase with the lattice velocity. With increasing laser beam intensities, the optical lattice potential depth increases and at relatively low gas densities a large number of gas particles can be trapped and collisionless accelerated.

When the gas density is high enough so that the mean collision time is much smaller than the pulse duration, it is not possible to effectively trap particles and accelerate them to high velocities with the lattice; it is still possible

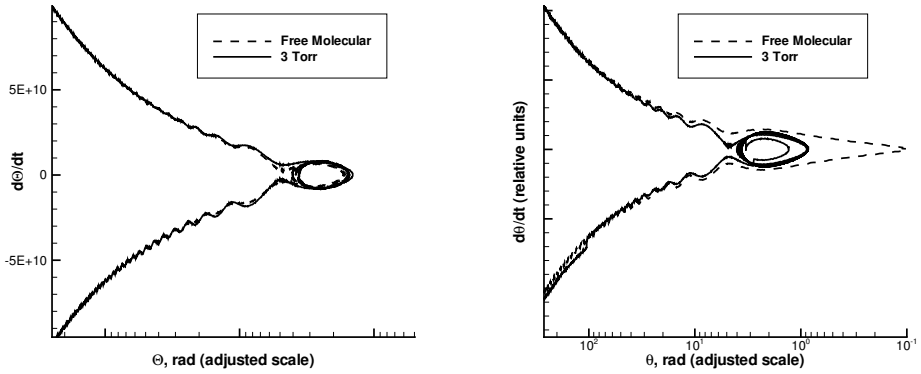

FIGURE 1. Phase diagrams for two particles in free molecular and collisional regimes.

however to increase the particle thermal velocity as well as transfer momentum from the lattice to the gas. In this case, the chirping of the lattice is not needed, and a constant lattice velocity should be used.

PARTICLE TRAPPING AND ACCELERATION IN WEAKLY COLLISIONAL REGIME

To study the effect of collisions on particle velocities in optical lattice, computations have been performed for a pure methane carrier gas perturbed by an optical lattice field. An 800 nm laser pulse intensity with a Gaussian temporal profile, a peak intensity of 1.3×10^{13} W/cm^2 and a FWHM pulse duration of 10 ns was used in the simulation. An initial lattice velocity of -6.5 km/s, and a chirp of 10^{19} rad/s^2 was used. The flow was computed in one dimension, assuming no potential in radial direction, and periodic boundary conditions at the inflow boundaries. Gas was initially stagnant at a temperature of 300 K. Two gas pressures were considered, 10^{-5} torr (free-molecular flow) and 3 torr. For the latter case, the gas is in a weakly collisional regime. For these pressures, this laser pulse is well below the breakdown. The initial simulated particle population was the same in these two cases, which allowed us to examine the trajectories of the same particles with and without collisions.

The velocity phase diagrams obtained in DSMC computations presented in Fig. 1 for two selected molecules and two pressures under consideration. The trajectory of a trapped molecules is given in Fig. 1a (dashed line). It is clearly seen that the molecule becomes trapped, and while being trapped its phase velocity oscillates around a stable point. After the laser intensity decreases, the potential well becomes shallow, and the molecule exits the well and becomes untrapped. The trajectory of the same molecule in the collisional case (solid line) shows that it collided at some early time moment before trapping, and as the result its phase velocity changed and the molecules was not trapped. Particle collisions, changing molecular velocities, may also lead to the trapping of particles that would not have been trapped without collisions. This is illustrated in Fig. 1b. In the free molecular regime, the considered molecule is not trapped. For a pressure of 3 torr, this molecule experienced a collision that changed its velocity so that is became trapped by the lattice.

The molecular velocities in the direction of the lattice acceleration as a function of the phase coordinate (relative to the accelerating lattice) are presented in Fig. 2 for trapped molecules at the two pressure regimes. The first molecule, Fig. 2a, was not disturbed by a collision during its trapping and acceleration. This resulted in an increase of the particle velocity to almost 12 km/s over the pulse period. The collision occurred for the 3 torr case close to the end of the pulse, which resulted in the instantaneous velocity decrease to about 1 km/s. The trajectory of a particle that experiences a collision during its trapping and acceleration is illustrated in Fig. 2b; the velocity drops from 9 km/s to about 5.5 km/s due to the collision. Note that since particles of the same mass collide, all collisions are relatively strong, and particles that collide while trapped usually become untrapped.

The situation is different if a trapped heavy molecule collides with surrounding light molecules, since in this case the velocity does not change significantly, and it may still be kept by the lattice. This was demonstrated in the computations performed for a gas mixture of 99% He and 1% Xe.

To study the effect of a pulsed lattice on the velocity distribution functions at different pressures, one-dimensional

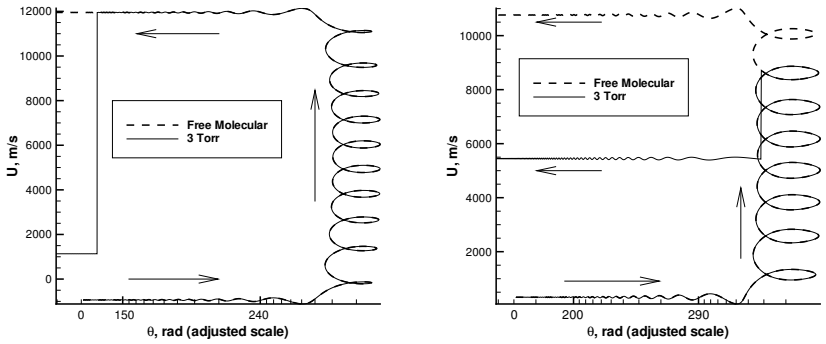

FIGURE 2. Velocities of two trapped molecules in the free molecular and transitional regimes.

computations have been performed . The test gas of methane was used which was initially stagnant at 300 K. The molecular distribution function of the gas at the end of the pulse is shown in Fig. 3 for two pressures, 0.01 torr, which is an essentially collisionless regime over the pulse duration, and 3 torr case where the mean collision time of about 17 ns is comparable to the pulse duration.

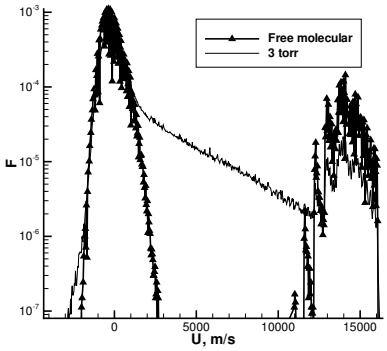

FIGURE 3. The velocity distribution function for methane gas at two pressures for an accelerating lattice.

In the absence of molecular collisions, the molecules that are being trapped in the potential well of the lattice can escape the well only after the laser intensity decreases enough. All of them acquire the lattice speed and are significantly accelerated. As a result, a bimodal distribution function is observed by the end of the pulse formed by untrapped molecules peaked at zero velocity and trapped molecules peaked at 14 km/s. The distribution function between the peaks is 0.

When molecular collision time becomes close to the pulse duration, the collisional relaxation causes a three-fold degradation of the trapped molecules peak. The collisions of trapped and untrapped molecules produce a distribution of molecules with velocities between 0 and 14 km/s.

ENERGY AND MOMENTUM DEPOSITION IN COLLISIONAL REGIME

In order to verify theoretical predictions and associated assumptions, and provide more detail on energy and momentum deposition, 1D DSMC computations have been performed for the following laser parameters. The laser pulse duration was 1 ns, the maximum single laser beam intensity was 0.25×10^{17} W/m^2 and 0.5×10^{17} W/m^2, the optical lattice wave length was 400 nm, and a Gaussian temporal profile of intensity was used with a maximum at 1 ns. The lattice velocity was varied from 0 to 1,500 m/s. The gas was methane, stagnant at $T_0 = 300$ K, and four pressures from 3 torr to 10 atm were considered.

The energy and momentum deposition per molecule is presented in Fig. 4 as a function of the lattice velocity for $I_{max} = 0.5 \times 10^{17}$ W/m^2. The momentum is normalized by the molecular mass. Several conclusions can be drawn from these figures. First, the values of velocity at which maximum energy deposition occursvalues are close to those predicted analytically. Second, the energy, as well as momentum, deposition per molecule slightly increases with pressure. The third conclusion is that the energy and momentum deposition are generally less efficient for 10 atm than for lower considered pressures at high lattice velocities. This is related to the fact that the quick maxwellization at 10 atm, when the collision time is over an order of magnitude shorter than the pulse duration, acts to prevent the deposition as compared to the velocity distribution that has a plateau formed due to the optical Landau damping[4] at lower pressures. This is confirmed by the fact that deposition at high lattice velocities becomes relatively more efficient for shorter pulses.

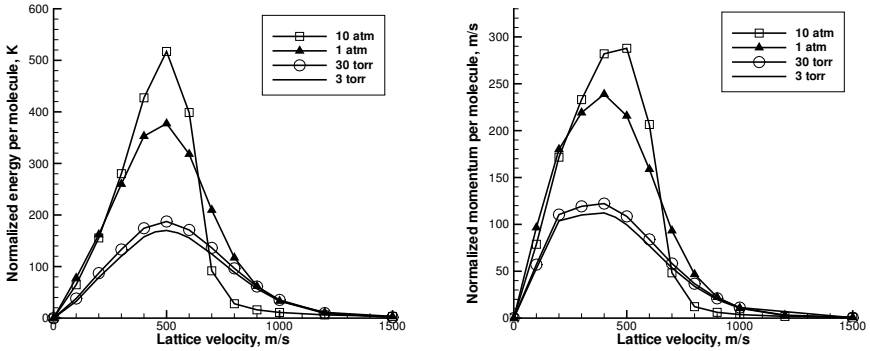

FIGURE 4. Energy and momentum deposition in an initially stagnant gas for different pressures and a long pulse with $I_{max} = 0.5 \times 10^{17}$ W/m^2.

The above computations show that it is possible to increase temperature of stagnant gas by a few hundred K if a nanosecond pulse is applied. The temperature increase may be much more significant if shorter (picosecond) and more intensive pulses are used to create an optical lattice. This is clearly shown in Fig. 5a where an increase in gas translational temperature due to an optical lattice formed by two 50 ps laser pulses at $I = 10^{18}$ W/m^2 and zero phase velocity is given. Two gases are considered here, methane and nitrogen; initially they are at 1 atm and 300 K and have no flow velocity. According to the estimates of high-intensity limits of breakdown for neutral molecules[5], the above laser intensity is at the breakdown threshold for methane, and still lower than the breakdown for nitrogen. The after-pulse temperature increases by 2000 K for methane and 1000 K for nitrogen; the higher temperature for methane is related to an almost three times larger polarizability-to-mass ratio. The ability of an optical lattice to increase gas temperature to thousands of K is comparable to that employed in the infrared laser powered pyrolysis [6] that is being widely used to study initiation and development of chemical reactions and various relaxation processes. Note also that gas temperature may be increased to significantly higher values if polarized molecules, such as water, are used. The increase in the laser beam intensity results in significantly stronger momentum deposition to the gas (see Fig. 5b). In this case, the gas velocity reaches 1000 m/s for methane at the phase velocity of $V_0 = 2000$ m/s. The value of $V_0 = 2000$ m/s is much higher than that predicted in Sec. II for small laser intensities; this is related to the fact that velocity distribution function significantly widens during the pulse, therefore increasing the associated thermal velocity.

ACOUSTIC SIGNALS INDUCED BY OPTICAL LATTICES

The results of the previous section demonstrate the ability of an optical lattice to effectively deposit momentum and energy into gas molecules. It would be highly desirable to compare these results with experimental measurements, and thus validate the theoretical approach and numerical models used. Experimental data on transient flow properties inside an optical lattice are currently unavailable, and obtaining them is a obviously very difficult task; it is much easier to examine the propagation of acoustic perturbations caused by a lattice, at some distance from its center. Measurements of an acoustic signal at different locations from the lattice would provide excellent ground for studying the lattice-gas interaction and numerical prediction validations.

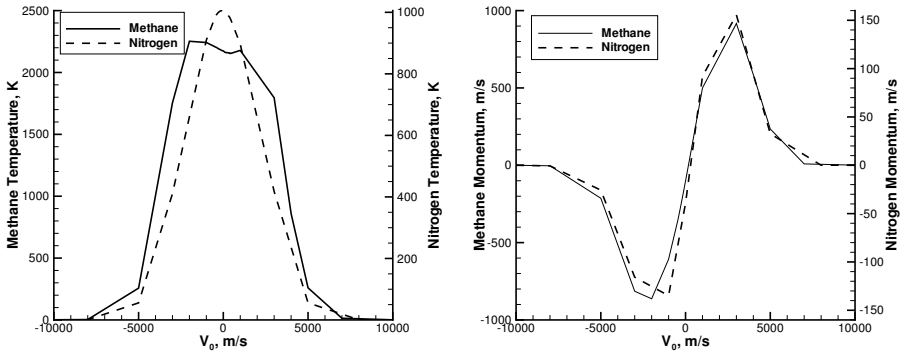

FIGURE 5. Translational temperature and momentum increase in an initially stagnant gas after a short pulse with $I_{max} = 10^{18}$ W/m^2.

In what follows, the initial stage of the evolution of a flow affected by an optical lattice and the development of acoustic perturbations is evaluated numerically. Axisymmetric DSMC computations have been performed where macroparameters in cells were recorded versus time. Over 160 million simulated molecules were used in order to maintain sufficiently low level of statistical fluctuations (the error associated with the statistical scatter is below 0.5%). The after-pulse transient pressure variation in the center of the lattice and at 1 mm in the radial direction is shown in Fig. 6a. Gas is nitrogen with initial pressure of 0.1 atm, temperature 300 K, and zero flow velocity. The laser pulse parameters are $I_{max} = 10^{18}$ W/m^2, $V_0 = 0$, the wave length is 800 nm, the beam diameter is 50 micron, and the Gaussian pulse duration is 50 ps. The coordinate of $Y = 0$ corresponds to the lattice centerline. The pressure at the center of the lattice quickly decreases in the first 300 ns after the pulse due to the expansion and diffusion of high-velocity molecules created by the lattice, which results both in temperature and density decrease at that time. The over-expansion of these molecules results in pressure decrease to values lower that the initial value of 0.1 atm. This is also clearly seen in Fig. 6b where the corresponding density profiles are shown. The pressure at the radial station of $Y = 0.975$ mm oscillates near its equilibrium value during the first 2 μs after the pulse; after that, there is a clear perturbation that correspond to an acoustic signal caused by the lattice. Note that the mentioned small fluctuations at $Y = 0.975$ mm are due to statistical scatter. For $Y = 0$, though, the fluctuations at $t > 3\mu$s are clearly stronger than the statistical noise, and are attributed to residual after-pulse flow oscillations near the lattice centerline. The density oscillations at $t > 3\mu$s are also noticeable (Fig. 6b).

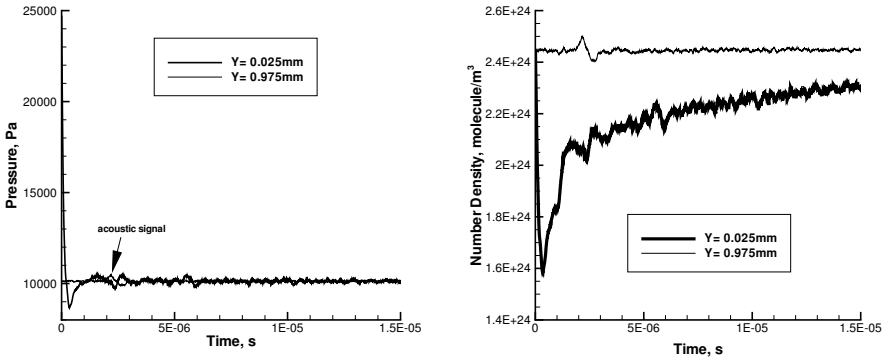

FIGURE 6. Pressure (a) and number density (b) as a function of time at two radial locations.

The propagation of an acoustic signal created by the lattice is clearly seen in Fig. 7a where the pressure is shown as a function of time at several radial stations. The signal reaches $Y = 0.525$ mm at a time of about 0.8 μs, which corresponds to the average signal speed of about 650 m/s, and effective gas temperature of about 1000 K. The temperature decrease downstream from the lattice center results in the decrease of the acoustic signal speed; the

average speed is about 500 m/s when it reaches 1 mm (see Fig 6a).

The results results presented above were obtained with the equilibrium free stream boundary conditions to approximate the acoustic signal development in a free space. If a gas cell is studied where the target gas is bound by solid walls, the acoustic signal will experience multiple reflections on these walls. The first of these reflections is illustrated in Fig. 7b where the pressure versus time is shown at $Y = 0.025$ mm for two boundary conditions, solid wall and equilibrium free stream (without wall). The acoustic signal reflected on the wall returns back to the centerline at about 5 μs, which corresponds to an average signal velocity of 400 m/s, and an effective temperature of 375 K.

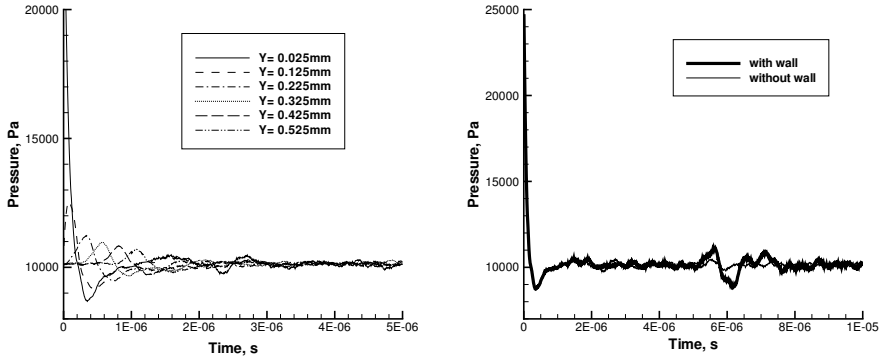

FIGURE 7. (a) Pressure at different radial locations. (b) Pressure in the center of the lattice for bounded and unbounded gas cell.

CONCLUSIONS

The effect of high intensity optical potentials on atomic and molecular gases is studied with the DSMC method. The trajectories of different atoms and molecules in the phase velocity space and molecular velocity space are examined both in the free molecular and collisional regimes. Trapping of particles by optical lattices in a collisional regime obtained in a numerical simulation is shown for the first time.

The deposition of energy and momentum from an optical lattice to a stagnant can be increased significantly for shorter and stronger pulses, shorter laser wavelengths, or, especially, if polarized molecules such as H_2O are used. Since only a small fraction of laser energy is deposited to gas, the use of a multi-pass optical system, with two laser beams being recycled many times, is also expected to produce significantly higher temperatures.

The formation and development of an acoustic signal created by the lattice is studied. The DSMC method was shown to be able to capture both the travel of an acoustic signal in high-density gases and after-pulse flow oscillations observed near the center of the lattice.

ACKNOWLEDGMENT

CN and SG were supported in part by the Propulsion Directorate of the AFRL at Edwards Air Force Base, California.

REFERENCES

1. Barker, P.F., and Shneider, M.N. "Optical microlinear accelerator for molecules and atoms," *Phys. Rev. A*, **64** (3) (2001)
2. Bird, G.A. *Molecular Gas Dynamics and the Direct Simulation of Gas Flows.* Clarendon Press, Oxford, 1994.
3. Ivanov, M.S., Markelov, G.N., and Gimelshein, S.F. "Statistical simulation of reactive rarefied flows: numerical approach and applications," AIAA Paper 98-2669.
4. Shneider, M.N., and Barker, P.F. "Optical Landau damping," *Phys.Rev. A*, **71**(5) (2005)
5. Dietrich, P. and Corkum, P.B. "Ionization and dissociation of diatomic molecules in intense infrared laser fields," *J. Chem. Phys.*, 97(5) 3187 (1992)
6. Russel, D.K., "Infrared laser powered homogeneous pyrolysis," *Chem. Soc. Rev.* **19**, 407 (1990)